

Bistable chaos without symmetry in generalized synchronizationShuguang Guan,^{1,2} C.-H. Lai,³ and G. W. Wei⁴¹*Temasek Laboratories, National University of Singapore, 5 Sports Drive 2, 117508 Singapore*²*Department of Computational Science, National University of Singapore, 117543 Singapore*³*Department of Physics, National University of Singapore, 117543 Singapore*⁴*Department of Mathematics, Michigan State University, East Lansing, Michigan 48824, USA*

(Received 26 March 2004; revised manuscript received 23 June 2004; published 17 March 2005)

Frequently, multistable chaos is found in dynamical systems with symmetry. We demonstrate a rare example of bistable chaos in generalized synchronization (GS) in coupled chaotic systems without symmetry. Bistable chaos in GS refers to two chaotic attractors in the response system which both synchronize with the driving dynamics in the sense of GS. By choosing appropriate coupling, the coupled system could be symmetric or asymmetric. Interestingly, it is found that the response system exhibits bistability in both cases. Three different types of bistable chaos have been identified. The crisis bifurcations which lead to the bistability are explored, and the relation between the bistable attractors is analyzed. The basin of attraction of the bistable attractors is extensively studied in both parameter space and initial condition space. The fractal basin boundary and the riddled basin are observed and they are characterized in terms of the uncertainty exponent.

DOI: 10.1103/PhysRevE.71.036209

PACS number(s): 05.45.Xt, 47.52.+j, 82.40.Bj

I. INTRODUCTION

A central problem in nonlinear dynamics is to explore how the asymptotic properties of a dynamical system evolve as the control parameter is continuously changed. The multistability of dynamical systems, i.e., the coexistence of more than one attractor for a given set of parameters, has attracted much research interest. It is known that in these systems the dynamics may sensitively depend on both the parameters and the initial conditions. This so-called “final state sensitivity” [1] implies that even the qualitative asymptotic behavior of the system cannot be predicted. In other words, given the initial conditions, in principle we do not know on which attractor the dynamics will finally settle down. The interesting dynamical phenomena related to the multistability and the final state sensitivity, such as fat fractals [2], fractal basin boundary [3], basin boundary metamorphoses [4], riddled basins [5], intermingled basins [6], and symmetry-breaking or increasing bifurcation [9,11,13,14,19,24], have been extensively studied.

So far, the multistability has been studied in both the map systems [7–16] and the flow systems [17–24]. Frequently, it is observed in dynamical systems with certain symmetry [9–16,19–24]. However, this does not imply that symmetry is a necessary condition for multistability. There are systems without symmetry which can exhibit multistability [7,8,17,18], mainly the coexistence of different periodic orbits or the coexistence of periodic orbit and chaotic attractor. In our opinion, the multistability is somewhat trivial if there exists symmetry in the dynamical equations, since in this case we can deduce that due to the symmetry mathematically it is possible for the system to exhibit multistability [23]. Therefore, multistability arising from the asymmetric dynamical systems deserves further attention.

Among the studies on multistability, the multistable chaos, i.e., the coexistence of more than one chaotic attractor, is particularly interesting since the chaotic attractor is the nontrivial one. As far as multistable chaos in flow systems is

concerned, we notice that the existing works all concentrate on the dynamical systems with certain symmetry [19–24]. To our knowledge, the multistable chaos in flow systems without symmetry has not been reported yet. However, we believe that it should exist in certain asymmetric dynamical systems. Recently, in the course of studying generalized synchronization (GS) [27–34] in coupled chaotic systems, we found an interesting example of bistable chaos which occurs in a dynamical system without any symmetry. The purpose of this paper is to report this finding, as well as the related bifurcations, such as GS and crisis, in the model studied. The significance of our work comes from the following two aspects. First, in contrast to the previous works on bistable chaos in flow systems with symmetry, the present study provides an uncommon example which is able to exhibit bistable chaos without any symmetry in the flow system. Our study thus broadens the research domain of bistable chaos in flow systems. Secondly, the model studied is a typical coupled dynamical system in which GS has been extensively studied previously [29–31], however the bistability in this model has not been pointed out so far.

We investigate one prototype dynamical model in GS, where the Lorenz system is uni-directionally driven by the Rössler system. This is the typical drive-response configuration [28–31]. In fact, our motive to study multistability in coupled chaotic systems was inspired by the work in Ref. [23], where the multistable chaos has been studied in the framework of GS. The key point in Ref. [23] is that there exists symmetry in the system’s equations such that multiple synchronization attractors which are related to the system’s symmetry can coexist in the response system. In our study, by choosing appropriate coupling, the inherent symmetry of the Lorenz system can be either kept or broken. Using the coupling strength as the control parameter, the bifurcations in the response system are explored for both the symmetric and the asymmetric models. In the symmetric case, as expected, bistable chaos is observed in GS, i.e., two chaotic attractors coexist in the response system which are both synchronized

with the drive system in the sense of GS. Surprisingly, it is further shown that this bistability in GS can even persist in a wide parameter range when the system's symmetry is broken by a different coupling scheme. The mechanism of the bistable chaos without symmetry is related to the crisis in the response system under chaotic driving. As a consequence of bistability, the fractal basin boundary and riddled basin are observed for certain parameter values. The fractal basin boundary is quantitatively characterized in terms of the uncertainty exponent [1,3].

In the present model, there is only one attractor in the response system without coupling. The bistability is the result of the chaotic driving, together with the special properties of the Lorenz system [25], for example its special topological structure in phase space. We emphasize that this bistability is essentially different from certain trivial situations. For example, it is known that due to symmetry the Lorenz system may have one symmetric attractor or a pair of bistable nonsymmetric attractors, depending on the parameters [25]. For certain parameters, two bistable periodic orbits can be generated through a symmetry-breaking bifurcation [26]. If with these parameter values the Lorenz system is driven by the Rössler system, we found that the bistability in GS can be observed in both the z coupling scheme (the symmetric case) and the x coupling scheme (the asymmetric case). However, we regard this bistability as a trivial one since without chaotic driving the system already exhibits bistability. On the other hand, we found that even when a dynamical system shows bistability (without driving), this bistability could be destroyed in the GS regime under the chaotic driving. For example, we have studied the model where the Duffing system in the bistable regime [19] is driven by the Rössler system. We found that the bistability no longer persists under the driving in the coupled systems.

This paper is organized as follows. In Sec. II, GS in coupled chaotic systems with symmetry is considered. We show that the model exhibits two types of bistability in GS, namely the type I and the type II bistability. In Sec. III, we further explore the asymmetric model where the system's symmetry is broken by choosing a different coupling scheme between the drive and response system. In both Sec. II and Sec. III, the bifurcation diagram is carefully explored using the coupling strength as the control parameter. In addition, the dependence of the bistable GS attractors on the parameters and the initial conditions is also extensively studied. The fractal basin boundary and riddled basin are observed, and the corresponding fractal dimensions are obtained by calculating the uncertainty exponents. At the end of this paper, there are concluding remarks.

II. BISTABILITY IN GS IN SYMMETRIC SYSTEM

The current study of bistable chaos is in the framework of GS, which is an important type of chaotic synchronization [27–34]. In GS, instead of the coincidence of two dynamics as in complete synchronization (CS), the dynamics of two chaotic systems are related by a certain functional relation. In fact, due to the parameter mismatch and the environment noise in practice, in the strict sense the observed chaos syn-

chronizations all belong to the domain of GS. Therefore, GS currently is under intensive investigation.

In the present model, GS occurs between two coupled chaotic systems [28–31]. The equations of the drive system are

$$\begin{aligned} \dot{u} &= -\alpha(v+w), \\ \dot{v} &= \alpha(u+av), \\ \dot{w} &= \alpha[b+w(u-c)], \end{aligned} \quad (1)$$

and the response system is governed by

$$\begin{aligned} \dot{x} &= \sigma(y-x), \\ \dot{y} &= rx-y-xz, \\ \dot{z} &= xy-\beta z-\epsilon(z-w). \end{aligned} \quad (2)$$

Here, the Lorenz system is unidirectionally driven by the Rössler system through the coupling term in the z variable. The time scaling factor α in Eqs. (1) is introduced to control the characteristic time scale, or to adjust the natural frequency of rotation of the Rössler oscillator [31]. The parameters are set as $a=b=0.2$, $c=5.7$, $\sigma=16$, $r=45.92$, and $\beta=4$. Without coupling, the Lorenz equations are invariant under the transformation $T:(x,y,z) \rightarrow (-x,-y,z)$, i.e., it has the symmetry of line inversion with respect to the z axis, or equivalently it has the symmetry of inversion in the xy plane. Apparently this symmetry is not affected in the above drive-response configuration since the driving signals are coupled to the z variable in the response system. Thus we call this situation the symmetric configuration.

We first explore the GS bifurcation between system (1) and system (2), which can be characterized by the negativity of the largest conditional Lyapunov exponent (LCLE) in the response system [27,29,31]. With negative LCLE, the response system becomes asymptotically stable and trajectories from different initial conditions will converge. We notice that due to the attractor bubbling [33], the standard synchronization criterion cannot always guarantee the high-quality synchronization in experiments or simulations [34]. Therefore, in the present study we also use the response-auxiliary system approach [30] to detect the occurrence of GS. In order to avoid misleading results using this approach, two issues are crucial in the numerical experiments. First, in the case of bistability we have to ensure that the initial conditions of the response system and the auxiliary system are in the same basin of attraction. Secondly, in the present study, a crisis occurs very near the GS bifurcation point. Thus a very long transient time should be thrown away near the GS bifurcation point. In our numerical experiments, the integrations are carried out up to 2×10^7 . The first period of 10^7 is discarded. The second period of 10^7 is analyzed to determine whether the GS or the crisis occurs. This convention is followed throughout this paper.

In the present model, α and ϵ are the two major parameters of interest. It is found that the time scaling parameter α has little influence on the GS bifurcation point. In fact, it

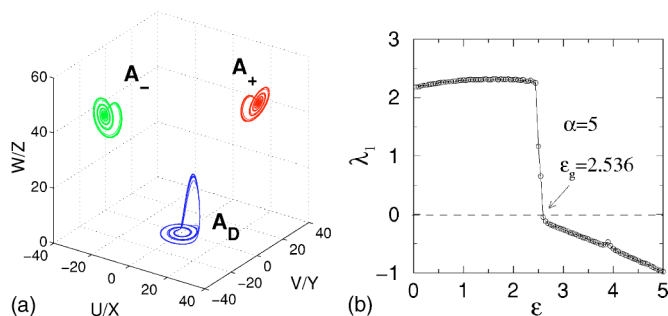


FIG. 1. For the symmetric model Eqs. (1) and (2). (a) The symmetric pair of bistable GS attractors A_+ and A_- in the response system as well as the driving attractor A_D . $\alpha=5$, $\epsilon=9$. (b) The LCLE of the response system λ_1 vs the coupling strength ϵ . $\alpha=5$.

mainly affects the phase of system (1). Usually when the coupling strength exceeds a critical value ϵ_g , which is numerically found between 2 and 3, the GS between the drive and the response system is achieved. What makes this GS special is that the response system exhibits bistability in GS. Here the bistability in GS refers to the fact that without driving there is only one attractor in the response system, while after GS there are two attractors in the response system, both of which synchronize with the driving dynamics. These two attractors are thus called the bistable GS attractors. Depending on the initial conditions, the system may evolve onto either of the bistable GS attractors. We emphasize that although the GS in the above model has been extensively studied previously [29–31], the bistability in GS in this model seems to have attracted little attention. In Fig. 1(a), we show a pair of typical bistable GS attractors as well as the driving Rössler attractor. It is found that in the xy plane, the attractor A_+ is confined in the first quadrant ($x > 0$ and $y > 0$) while the attractor A_- is always in the third quadrant ($x < 0$ and $y < 0$). They form a symmetric pair under the transformation $T: (x, y, z) \rightarrow (-x, -y, z)$, but neither of them is symmetric under such transformation. Interestingly, it is seen that under the driving, the topological structures of bistable GS attractors A_+ and A_- resemble that of the driving attractor A_D . As shown in Fig. 1(a), they rotate around a center in a plane for a period of time, then burst and escape from the rotation plane in the transverse direction for a while, and finally return onto the plane to go on with the rotation, and so on.

In the present study, the GS accompanies the qualitative change of the attractor in the response system. The qualitative changes of chaotic attractor in phase space, such as the sudden change in the size of the chaotic attractors and the sudden appearance of chaotic attractors, have been known as the crisis bifurcation. In crisis, the chaotic attractor may collide with the unstable periodic orbit on the basin boundary that separates them [20,35]. In dynamical systems with symmetries, the appearance or disappearance of a pair of bistable chaotic attractors is frequently observed [9,11,13,14,19,24]. Therefore, it is not strange to observe the bistability in GS in the symmetric model. One important feature of the crisis in the current model is that the control parameter, i.e., the coupling strength, is a parameter reflecting the magnitude of the chaotic driving from the drive system. This implies that the

crisis in the response system is caused by the chaotic driving.

In order to understand the mechanism of the bistability, a qualitative study of the bifurcation diagram about the GS and the crisis is necessary. To this end, we now focus on the bifurcation processes in a concrete example at $\alpha=5$. With the increase of the coupling strength, the GS bifurcation first occurs at $\epsilon_g=2.536$, which is characterized by the LCLE in the response system in Fig. 1(b). On the other hand, Fig. 1(a) shows that the original single attractor in the response system has split into a pair of bistable attractors, which shrink drastically in phase space. This phenomenon is a typical signature of crisis. Therefore, both GS and crisis occur in the response system with large coupling strength. At first glance, it appears that the crisis occurs simultaneously with the GS bifurcation. However, a careful examination reveals that there are two crises occurring at different coupling strength. The first one takes place at ϵ_g , i.e., the GS bifurcation point, and the second one takes place at $\epsilon_c=2.623$, a little larger than the GS bifurcation point ϵ_g . Therefore, there are three parameter regimes for the control parameter ϵ . They are regime I ($\epsilon < \epsilon_g$), regime II ($\epsilon_g \leq \epsilon < \epsilon_c$), and regime III ($\epsilon \geq \epsilon_c$). In regime I, the response system does not synchronize with the drive system. Its attractor at this stage keeps the butterfly shape of the Lorenz attractor, although it is perturbed by the driving signals, as shown in Fig. 2(a). In regime II, GS is achieved and simultaneously the response system undergoes a crisis where the attractor unfolds to become two bistable attractors. At this stage, the bistable GS attractors still keep the shape of the Lorenz attractor, as shown in Figs. 2(b) and 2(c). The characteristic of the bistable attractors in this regime is that they totally overlap in phase space, but they have different basins of attraction. As shown in Figs. 2(d)–2(f), they are exactly related to each other by the system’s symmetry. The bistability in this regime is similar to the situation described in Ref. [23]. We believe it should be observed in many symmetric systems. We call this bistability type I bistability. In the current model, type I bistability has also been observed for other α values such as $\alpha=4$. Nevertheless, for other α values, such as $\alpha=1$ or $\alpha=6$, regime II is too narrow to be observed in our numerical experiments.

When $\epsilon \geq \epsilon_c$, the system enters into regime III, where the response system exhibits a different type of bistability in GS. Due to the crisis at ϵ_c , the overlapped bistable attractors suddenly shrink greatly and become two well separated attractors in phase space, as shown in Figs. 3(a)–3(c), as well as in Fig. 1(a) for a three-dimensional view. From Figs. 1(a) and 3(c), it is seen that the bistable attractors in this regime resemble the driving Rössler attractor. This is different from the situation in regime II. We thus refer to this bistability, where the symmetric pair bistable attractors are separated in phase space, as type II bistability. Type II bistability in GS has not been reported before.

In dynamical systems with multistability, the boundary between different basins of attraction is frequently fractal [1,3]. We investigate the dependence of the bistable GS attractors on both initial conditions and parameters. In our numerical experiments, if the dependence of the dynamics on initial conditions is studied, the parameters (α, ϵ) are fixed and the initial conditions go through the $z=0$ plane; if the

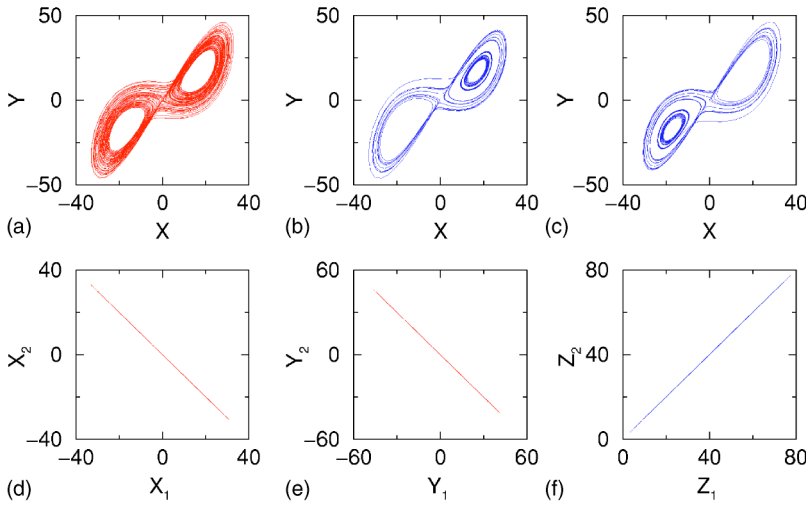


FIG. 2. Type I bistability in GS in the symmetric model with $\alpha=5$. (a) Attractor of the response system at $\epsilon=2.5$. At this stage there is no GS between the coupled systems. (b) and (c) Bistable GS attractors at $\epsilon=2.55$. For the visualization, we specially choose a short period of time so that the two attractors can be distinguished in phase space. For a long time, they are both like the attractor in (a). (d)–(f) The bistable GS attractors are symmetric under the inversion transformation in the xy plane, while identical in the z direction.

dependence of the dynamics on parameters is studied, the initial conditions of the response systems are fixed and the parameters α and ϵ go through the α - ϵ parameter plane. In both cases, the initial conditions in the drive system are fixed. The results are shown in Figs. 4 and 5. For type I bistability, it is found that the basins of the bistable GS attractors in the initial condition space are intermingled, as shown in Fig. 4. Usually, final-state sensitivity in both phase space and parameter space can be quantified by the uncertainty exponents γ [3]. The exponent γ is defined as follows. In phase space or parameter space, randomly choose a phase point r_0 . Define another phase point $r'_0=r_0+\delta$, where δ is a small perturbation. Determine whether the final states of the system using these two initial conditions or parameter values are on different attractors. If so, the initial conditions or the parameters are called uncertain initial conditions or uncertain parameter values. For a given perturbation δ , the fraction of uncertain initial conditions or uncertain parameter values, $f(\delta)$, can be calculated by randomly choosing many different initial conditions or parameter values. Typically there is a scaling relation, $f(\delta) \sim \delta^\gamma$, where γ is the uncertain exponent. In the plot of $\log f(\delta)$ versus $\log \delta$, the uncertainty exponent γ is just the slope of the straight line. It has been proven that

the uncertainty exponent δ and the basin boundary dimension satisfy the relation $\gamma=D-d$, where D and d are the dimension of the phase space and the basin boundary dimension, respectively [3]. In Fig. 4, the uncertainty exponents are computed using the above method, which confirm that the basins of attraction are riddled for type I bistable attractors. The error bars in Fig. 4 (also in Figs. 10 and 12) are determined in the same way as in Ref. [3]. For type II bistability, however, it is found that the basin boundaries are trivial curves in both the parameter space and the initial condition space. Two typical examples are shown in Fig. 5. It is pointed out that in the initial condition space, the basins of attraction of A_+ and A_- are symmetric under inversion transformation in the xy plane. This is also due to the symmetry in the response system. If from the initial point (x_0, y_0, z_0) the system will asymptotically settle on attractor A_+ , then from the initial point $(-x_0, -y_0, z_0)$ the system will definitely go to attractor A_- .

To conclude, in this section we investigated the bistability in GS when the response system has the line inversion symmetry $T:(x, y, z) \rightarrow (-x, -y, z)$. Two types of bistability in GS have been identified, i.e., type I and type II bistable chaos. The former occurs within the parameter regime II, where the

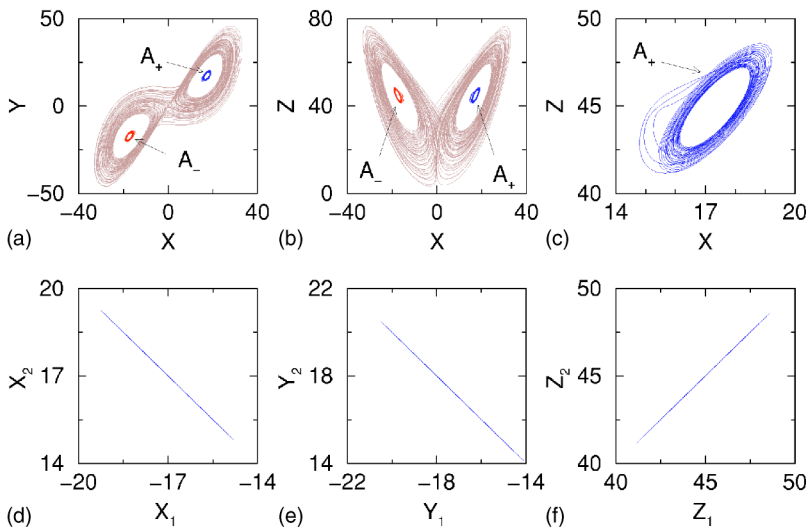


FIG. 3. Type II bistability in GS in the symmetric model with $\alpha=5$. (a)–(c) Attractors of the response system with different coupling strength. Two GS attractors A_+ and A_- at $\epsilon=2.7$ are shown in black. The attractor at $\epsilon=2.5$ before the crisis is also shown in gray for comparison of the attractor size before and after the crisis. Note that the scale of (c) is different from (a) and (b). (d)–(f) The two GS attractors are symmetric under the inversion transformation in the xy plane, while identical in the z direction.

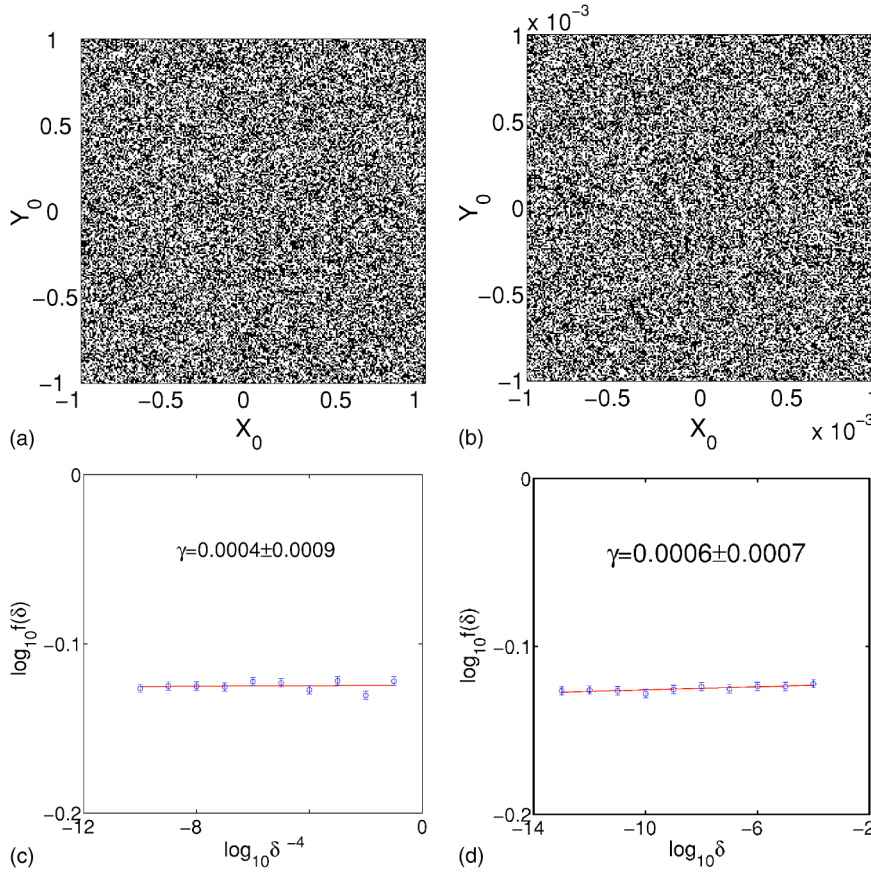


FIG. 4. (a) and (b) For type I bistability, the basins of attraction of the bistable GS attractors are intermingled on the $z=0$ plane. The white and black areas, respectively, denote the two basins of attraction. (b) is the enlargement of a small window on (a). Note that the origin must be excluded because the axis z , i.e., the line $x=0$ and $y=0$, is the invariant subspace of the dynamical system (2). $\alpha=5$, $\epsilon=2.6$. The initial conditions for the drive system are fixed as $(-1, -1, -1)$. (c) and (d) The uncertainty exponents for (a) and (b), respectively. γ is the slope of the straight line.

bistable GS attractors totally overlap in phase space. The latter occurs within the parameter regime III. The type II bistable GS attractors are well separated in phase space. Due to the system's symmetry, the bistable attractors for both type I and type II bistability form a symmetric pair. We believe these two types of bistable chaos are typical in symmetric dynamical systems.

III. BISTABILITY IN GS IN AN ASYMMETRIC SYSTEM

In general, if a certain phenomenon occurs in a symmetric system, it is of particular importance to ascertain to what extent such a phenomenon is related to the system's symmetry. It would be surprising if certain dynamical properties which exist in symmetric systems continue to exist even after such symmetry is broken. If this happens, we can conclude that the symmetry is not a necessary condition to generate the phenomenon. We notice that in flow systems, the existing studies on multistable chaos are carried out in symmetric systems [19–24]. Naturally, it is important to find out what would happen if the system's symmetry is broken. To this end, in this section we study a different drive-response configuration where the response system's symmetry is deliberately broken by choosing an appropriate coupling term. Interestingly, it is found that in this case the model still can exhibit bistability in GS in a wide range of parameters. Therefore, what we observe is a rare case of bistability without symmetry. Later we will show that although the bistable GS attractors have no simple symmetric relation in this case,

they are likely to have a certain functional relation between them.

We still consider GS in the drive-response configuration. The drive system is the same as Eqs. (1), and rewritten here

$$\dot{u} = -\alpha(v + w),$$

$$\dot{v} = \alpha(u + av),$$

$$\dot{w} = \alpha[b + w(u - c)], \quad (3)$$

but the response system has been changed to

$$\dot{x} = \sigma(y - x) - \epsilon(x - u),$$

$$\dot{y} = rx - y - xz,$$

$$\dot{z} = xy - \beta z, \quad (4)$$

where the driving signal is coupled to the x variable in the response system. All parameters are the same as in the previous section. Apparently, the inherent symmetry of the Lorenz system has been broken by this coupling term. We denote this model as the asymmetric model, in contrast to the symmetric model studied in the previous section.

A. The bifurcations

We first explore the bifurcation diagram of system (4) under the driving from system (3) with $\alpha=3$. With the in-

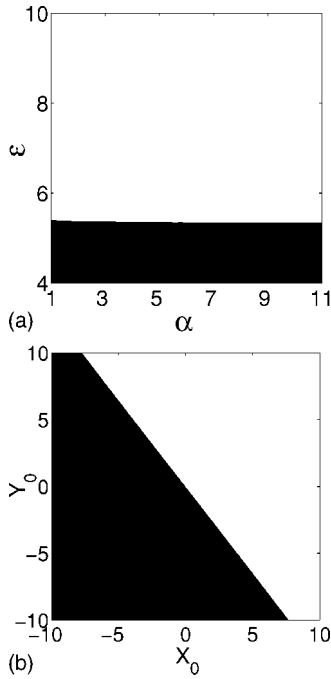


FIG. 5. The basins of attraction on the parameter plane and initial condition plane for type II bistability. The white and black are basins of attraction of A_+ and A_- , respectively. (a) The basins of attraction on the α - ϵ parameter plane. The initial conditions for the drive and the response systems are fixed as $(-1, -1, -1)$ and $(1, 1, 1)$, respectively. (b) The basins of attraction on the initial condition plane $z=0$. The parameters are fixed as $\alpha=5$ and $\epsilon=9$. The origin should be excluded for the reason mentioned in Fig. 4.

crease of the coupling strength, GS first takes place in the response system. Figure 6 characterizes the GS bifurcation by the LCLE in the response system. The critical coupling strength is $\epsilon_g=4.521$. Generally, it is found that the critical coupling strength for achieving GS in the asymmetric case is larger than that in the symmetric case. In both the symmetric and the asymmetric cases, the time scaling parameter α has little effect on the GS bifurcation point.

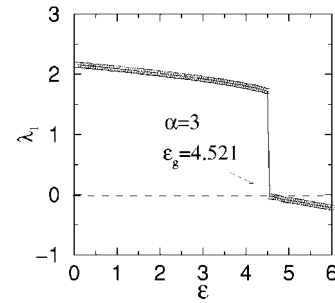


FIG. 6. For the asymmetric model Eqs. (3) and (4), $\alpha=3$. The LCLE of the response system λ_1 vs the coupling strength ϵ .

What makes the present study interesting is that the model can still exhibit bistability in GS even without symmetry. With the further increase of the coupling strength after the GS bifurcation, it is found that a series of crises successively occur. We numerically identified three crises which occur at $\epsilon_1=4.548$, $\epsilon_2=38.588$, and $\epsilon_3=48.523$, respectively. The GS bifurcation point and these three crisis bifurcation points divided the ϵ axis into five regimes.

In regime I, i.e., $\epsilon < \epsilon_g$, GS has not been achieved between two coupled systems. A typical attractor of the response system at this stage is shown in Fig. 7(a). In regime II, i.e., $\epsilon_g \leq \epsilon < \epsilon_1$, GS is achieved, but no bistability is observed in this stage. This is different from the situation in the symmetric model, where the GS bifurcation is a twofold one in the sense that GS and the bistability simultaneously happen. After that, the system enters into the bistable chaos regime. However, in the asymmetric model the bistability does not simultaneously appear with the GS bifurcation. In regime II, only one GS attractor is observed, as shown in Fig. 7(b).

The response system does not exhibit bistability until it enters regime III, i.e., $\epsilon_1 \leq \epsilon < \epsilon_2$. It is found that at ϵ_1 a crisis occurs, where the single GS attractor in regime II suddenly splits into two separated attractors. In the meantime, the newborn bistable attractors have greatly shrunk compared with the GS attractor in regime II. The bistability can be observed in the whole regime III, which is a relatively large

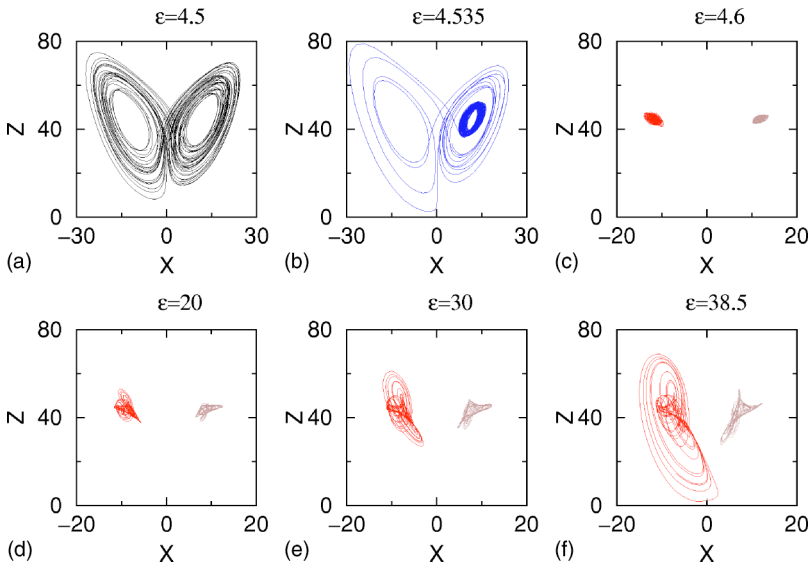


FIG. 7. The metamorphoses of the attractor in the xz plane in the response system with the increase of coupling strength. $\alpha=3$. The GS bifurcation occurs at $\epsilon_g=4.521$, and the three successive crises occur at $\epsilon_1=4.548$, $\epsilon_2=38.588$, and $\epsilon_3=48.523$, respectively. (a) GS has not been achieved at $\epsilon=4.5$ in regime I; (b) GS has been achieved, but there is no bistability at $\epsilon=4.535$ in regime II; (c)–(f) asymmetric bistable attractors (in black and gray, respectively) expand gradually at $\epsilon=4.6$, 20, 30, and 38.5 in regime III. In (b), the parameter is near the crisis point, thus the attractor spends a long time in the region in phase space where the bistable attractors will form after the crisis.

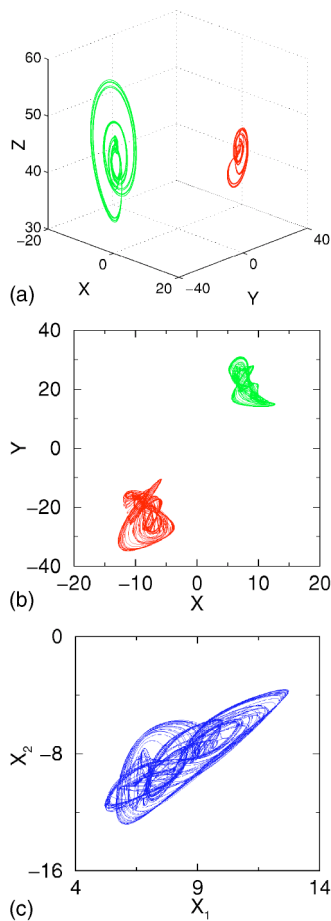


FIG. 8. (a) and (b) Typical asymmetric bistable GS attractors for type III bistability. $\alpha=3$ and $\epsilon=25$. (c) The mapping between two x variables of the drive and the response system.

parameter range. Thus we emphasize that this bistability is a robust phenomenon and cannot be regarded as a transient behavior. The evolution of the bistable GS attractors in regime III is shown in Figs. 7(c)–7(f). Similar to the symmetric case, in the xy plane one GS attractor is confined in the first quadrant while the other is in the third quadrant immediately after the crisis. However, in this situation the bistable GS attractors no longer have a symmetric relation. We denote this asymmetric bistability as type III bistability in order to distinguish from the type I and type II bistability in the symmetric model. With the increase of the coupling strength within regime III, it is found that the bistable GS attractors expand in phase space. Remarkably, attractor A_- expands faster than attractor A_+ , as seen in Figs. 7(c)–7(f). As a consequence of this unbalanced expansion, at certain relatively large coupling strength, attractor A_- first crosses the $x > 0$ region in phase space. Soon after this, it disappears in the second crisis at ϵ_2 . After the second crisis, there is no bistability in the response system.

In regime IV, i.e., $\epsilon_2 \leq \epsilon < \epsilon_3$, only one GS attractor A_+ exists, which continues to expand as the coupling strength increases. Finally, the third crisis occurs at $\epsilon_3=48.523$. This time, however, attractor A_+ does not disappear. Instead it suddenly doubles its size and becomes a double-scroll attractor that resembles the Lorenz attractor (not shown). There-

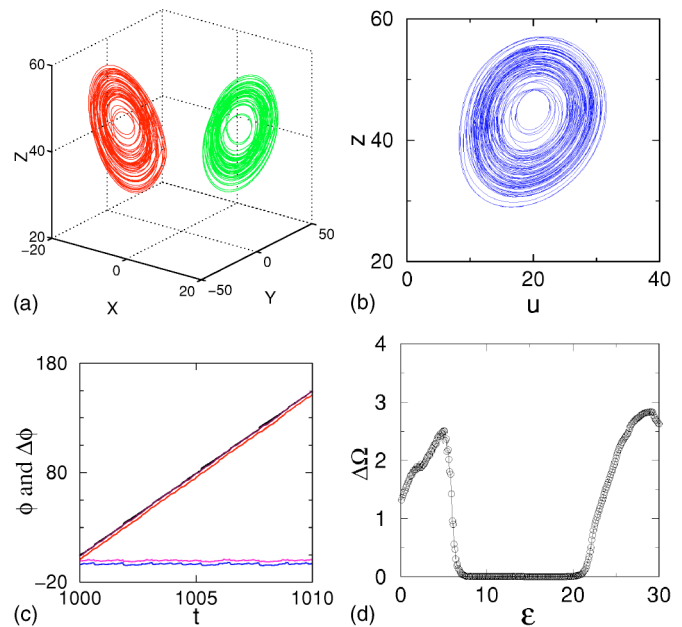


FIG. 9. PS between the bistable attractors and the drive system for type III bistability. $\alpha=14$ and $\epsilon=10$. (a) Three-dimensional plot of the bistable attractors. (b) One of the bistable attractors in the uz plane. (c) The phases of the drive system and the bistable attractors in the response system, as well as the phase differences between them. (d) The frequency difference between the drive system and one of the bistable attractors in the response system vs the coupling strength.

fore, the GS in regime V, i.e., $\epsilon_3 \leq \epsilon$, is similar to that in regime II.

Now different parameter regimes in the asymmetric model are clear. For regimes I–V discussed above, GS occurs in regimes II–V, while type III bistability in GS occurs in regime III. Comparing these results with that in the previous section, we conclude that all three types of bistabilities are caused by a crisis in the response system regardless of the system’s symmetry. The difference dictated by the system’s symmetry is whether the bistable GS attractors are symmetric or not.

B. The relation between bistable GS attractors

In the present study, the type III bistability, i.e., the bistable chaos in an asymmetric system, is quite remarkable. There are some features in the bistable GS attractors that are worth noting. First, in a wide parameter range, the bistable attractors are, respectively, confined in different quadrants on the xy plane, just as in the symmetric case. Secondly, they are no longer symmetric in phase space, and their expansion speeds in phase space are different as the coupling strength is increased. Thirdly, the mechanism of the asymmetric bistability is also due to the crisis, which turns out to be robust in the present model regardless of whether it has symmetry or not. In Fig. 8, a pair of typical asymmetric bistable GS attractors are plotted with the features discussed above. Although now there is no symmetric relation between them, we argue that there still exists a certain, perhaps complicated,

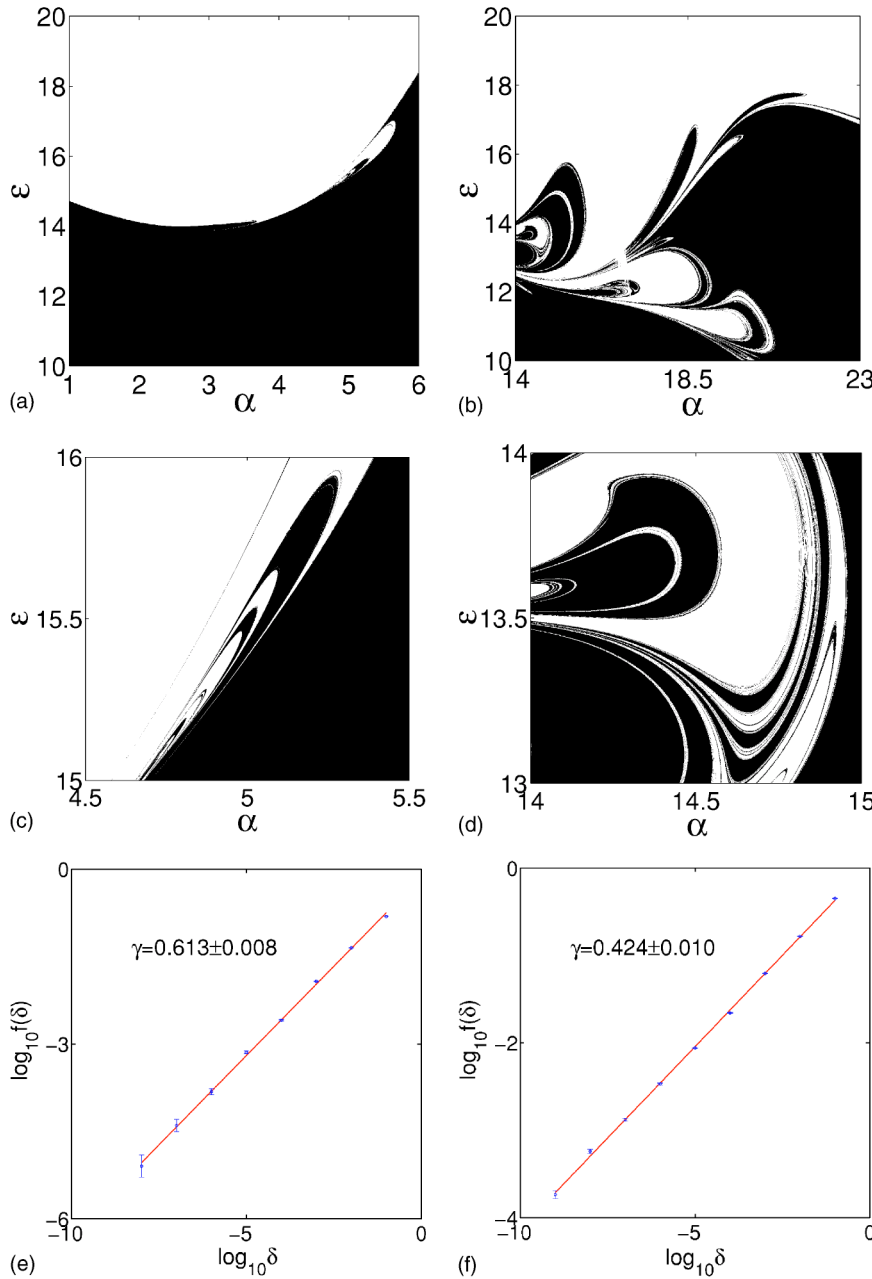


FIG. 10. (a) and (b) The basins of attraction of the bistable attractors on the parameter plane α - ϵ for type III bistability. The initial conditions of the drive and the response systems are fixed as $(-1, -1, -1)$ and $(1, 1, 0)$, respectively. (c) and (d) The blow-ups of (a) and (b) showing fractal basin boundaries. (e) and (f) The uncertainty exponents for (c) and (d), respectively. γ is the slope of the straight line.

relation between them. In Fig. 8(c), the mapping between the x variables of the bistable attractors seems to suggest this. In fact, because the bistable GS attractors both synchronize with the drive system, they both have certain functional relations with the drive system, i.e., due to GS, generally we have $A_+ = f(A_D)$ and $A_- = g(A_D)$. Following this, A_+ and A_- now could be related as $A_+ = f(A_D) = f(g^{-1}(A_-)) = h(A_-)$, where $h = fg^{-1}$, and we reasonably assume that g^{-1} exists as in common situations of GS [36]. Therefore, A_+ and A_- may have a functional relation given the GS relations between them and the driving attractor are invertible. From this perspective, they certainly can be regarded as synchronized in the sense of GS. Such special GS can be called indirect GS in order to distinguish from the usual GS.

Usually, GS is observed between different dynamical systems, which are either parametrically different or physically

different. Here a special situation is demonstrated where GS can be observed between two bistable attractors within one dynamical system. The prerequisite of such GS is that the two attractors in the response system are indirectly related by the same driving signals. We argue that the indirect GS among multiple attractors is a generic phenomenon in coupled chaotic systems as long as the system exhibits multistability under the same driving perturbations.

For phase-coherent dynamical systems, such as the Rössler system and the Lorenz system, a suitable phase of the dynamics can be defined [37,38]. It has been shown that two systems can achieve phase synchronization (PS) while their amplitudes may remain uncorrelated [37–39]. The existing studies of PS are mainly based on the coupled parametrically different systems, such as two Rössler systems, or two Lorenz systems. PS between two essentially different

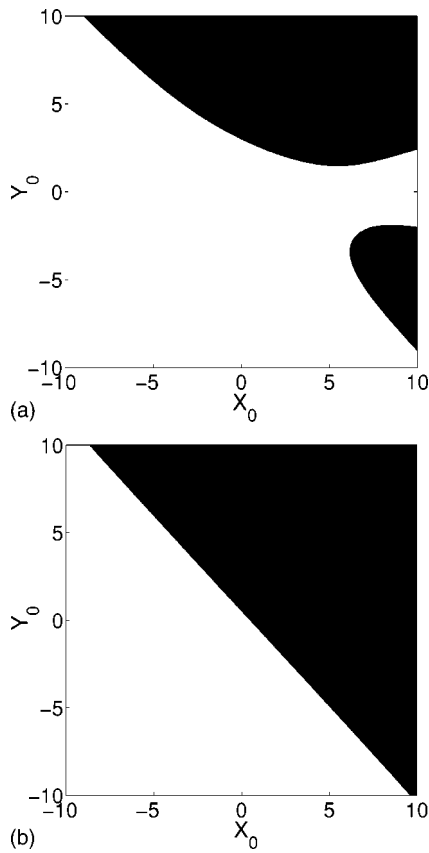


FIG. 11. The regular basin boundary of the bistable attractors in the $z=0$ plane for type III bistability at (a) $\alpha=1, \epsilon=15$; (b) $\alpha=2, \epsilon=10$, respectively. The initial conditions of the drive system are fixed as $(-1, -1, -1)$.

systems has not been addressed yet. In the present work, we also investigate the PS between the Rössler system and the Lorenz system, which are two essentially different systems. Since both systems are phase-coherent, it is reasonably expected that PS can be achieved between them. In our numerical experiments, we successfully observed PS between these two chaotic systems in a certain parameter range. In Fig. 9, an example is provided showing PS between system (3) with $\alpha=14$ and system (4). It should be pointed out that in this case the response system actually exhibits type III bistability. Two asymmetric bistable attractors are shown in Fig. 9(a). Following the convention [37–39], the phase of the Lorenz system can be defined in the uz plane, where $u = \sqrt{x^2 + y^2}$. One of the bistable attractors in the uz plane is shown in Fig. 9(b). The phase definition is straightforward,

$$\phi(t) = \arctan \frac{z(t) - z_0}{u(t) - u_0}, \quad (5)$$

where (u_0, z_0) is the rotation center which usually is one of the unstable fixed points of the system. Figure 9(c) plots the phases and the phase differences between the driving attractor and the bistable attractors in the response system, showing that phases are locking between them. Based on the definition of phase, the mean frequency of a chaotic system can be defined as

$$\Omega = \lim_{T \rightarrow \infty} \frac{1}{T} \int_0^T \dot{\phi}(t) dt. \quad (6)$$

In Fig. 9(d), the frequency difference between the drive system and one of the bistable attractors in the response system is plotted versus the coupling strength. It is seen that a PS plateau exists in the moderately large coupling strength range. We emphasize that since both the bistable GS attractors have the PS relation with the driving Rössler attractor, the bistable GS attractors are also synchronized with each other in phase.

C. The basin of attraction

In the symmetric case, as shown in Figs. 4 and 5, the basins of attraction of the bistable attractors are either riddled for type I bistability or trivial for type II bistability. When the system's symmetry is broken, the situation is different. The dependence of the type III bistability on parameters is illustrated in Fig. 10. It is found that when α is small, for example $\alpha < 3$, the basin boundary of the bistable GS attractors is still trivial. However, with the increase of α , this boundary would be fractal as shown in Figs. 10(a) and 10(b). The existence of infinitely fine-scaled structures is evident in Figs. 10(c) and 10(d). The dependence of the bistability on initial conditions has also been extensively investigated numerically. The results are shown in Figs. 11 and 12. Similar to the results on the parameter plane, the basin boundaries on the initial condition plane are also trivial when α is small, as shown in Fig. 11. However, for large α values, generally the basin boundary between the bistable attractors is fractal. Typical examples of the fractal basin boundaries are shown in Fig. 12. It is noted that these basins of attraction are no longer symmetric in both the trivial cases in Fig. 11 and the nontrivial cases in Fig. 12.

In order to quantitatively characterize these fractal basin boundaries, the uncertainty exponents have been computed [1,3]. The results are also shown in Figs. 10 and 12. In all these figures, the linear dependence of $\log f(\delta)$ on $\log \delta$ is evident. The uncertainty exponent γ is determined as the slope of the straight line. For the examples given in Fig. 12, the uncertainty exponents range from 0.374 to 0.510. Correspondingly, the boundary dimensions range from 1.626 to 1.490.

IV. CONCLUDING REMARKS

In this paper, we report on a study of bistable chaos in GS in coupled chaotic systems, where the Lorenz system and the Rössler system are coupled in a drive-response configuration. It is found that depending on the initial conditions, there are two attractors in the response system which both synchronize with the drive dynamics. By exploring both the symmetric and asymmetric models, we identified three types of bistable chaos. Among them, type I and type II bistability

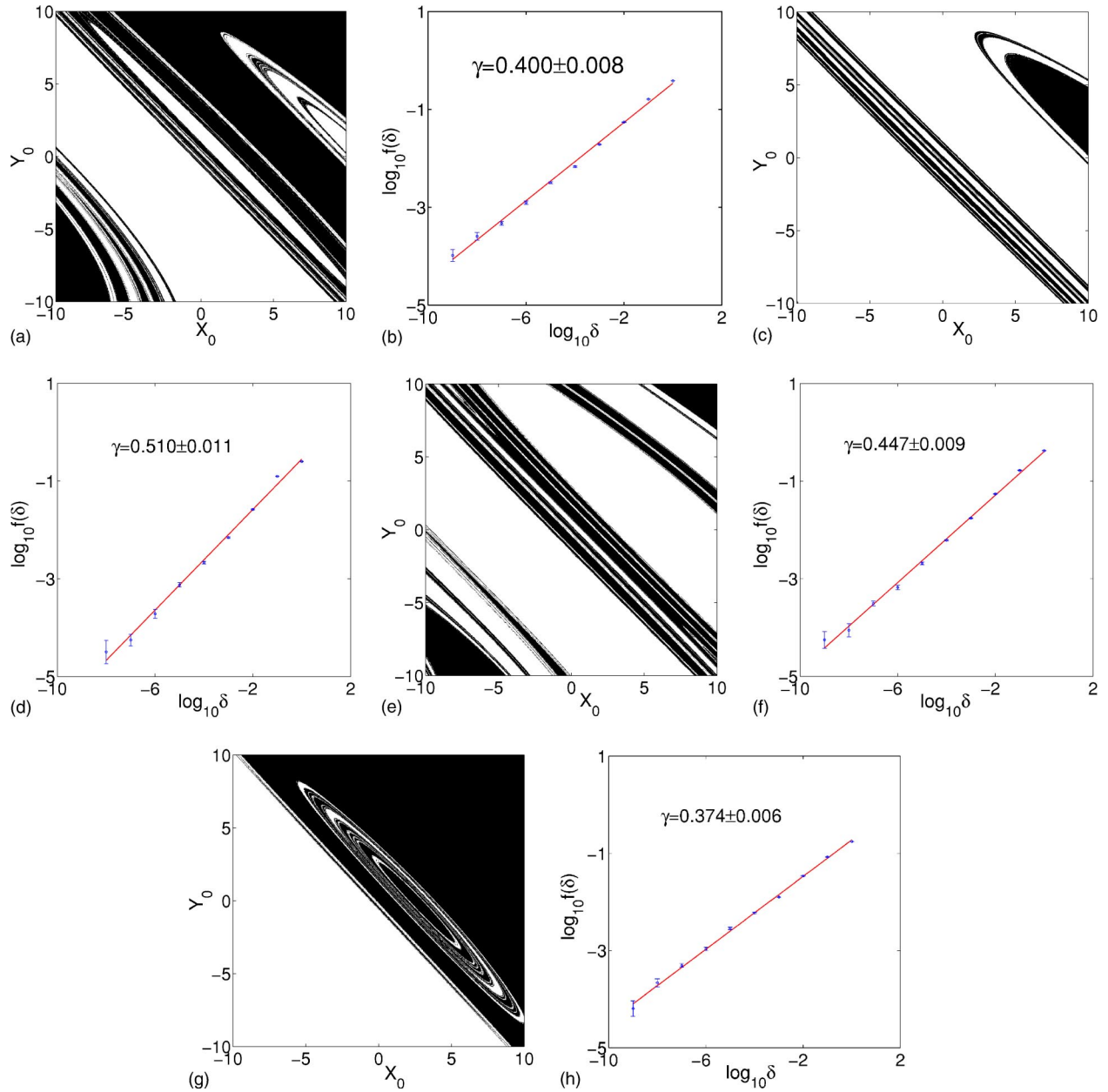


FIG. 12. The fractal basin boundary of the bistable attractors and the corresponding uncertainty exponent for type III bistability. (a) and (b) $\alpha=14, \epsilon=14$; (c) and (d) $\alpha=17, \epsilon=16$; (e) and (f) $\alpha=18, \epsilon=14$; (g) and (h) $\alpha=19, \epsilon=11$. The initial conditions of the drive system are fixed as $(-1, -1, -1)$.

occur in the symmetric model while the remarkable type III bistability occurs in the asymmetric model where there is no inherent symmetry in the system's equations. The mechanism for the bistability in the present study is revealed. It is the crisis in the response system under chaotic driving that leads to the splitting of the synchronous attractor and thus generates the bistability. The basin of attraction of the bistable attractors is characterized in both parameter space and initial condition space. Our findings in this work not only complement the previous study of GS in the model, but also enrich the study of multistability in asymmetric flow systems.

Finally, we would like to point out that although the situation studied in the current work is bistability and symmetry,

the results and discussion are generally suitable for dynamical systems with multistability.

ACKNOWLEDGMENTS

We thank Dr. B. S. V. Patnaik and Dr. M. Zhan for reading the manuscript and giving constructive comments. S.G. is grateful for the helpful discussions with Dr. X. Wang and Dr. X. Gong. This work was supported by the Temasek Laboratories at National University of Singapore and the Michigan State University. The authors would also like to thank the Department of Computational Science at National University of Singapore for the use of computational facilities.

- [1] E. Ott, *Chaos in Dynamical Systems* (Cambridge University Press, New York, 1993).
- [2] J. D. Farmer, Phys. Rev. Lett. **55**, 351 (1985); D. K. Umbarger and J. D. Farmer, *ibid.* **55**, 661 (1985).
- [3] C. Grebogi, S. W. McDonald, E. Ott, and J. A. Yorke, Phys. Lett. **99A**, 415 (1983); S. W. McDonald, C. Grebogi, E. Ott, and J. A. Yorke, Physica D **17**, 125 (1985).
- [4] C. Grebogi, E. Ott, and J. A. Yorke, Phys. Rev. Lett. **56**, 1011 (1986).
- [5] J. C. Alexander, J. A. Yorke, Z. You, and I. Kan, Int. J. Bifurcation Chaos Appl. Sci. Eng. **2**, 795 (1992); E. Ott, J. C. Sommerer, J. C. Alexander, I. Kan, and J. A. Yorke, Phys. Rev. Lett. **71**, 4134 (1993); Y. C. Lai and R. L. Winslow, *ibid.* **72**, 1640 (1994); Y. C. Lai, C. Grebogi, J. A. Yorke, and S. C. Venkataramani, *ibid.* **77**, 55 (1996).
- [6] Y. C. Lai and C. Grebogi, Phys. Rev. E **52**, R3313 (1995); M. Zhan and G. Hu, *ibid.* **62**, 375 (2000).
- [7] U. Feudel, C. Grebogi, B. R. Hunt, and J. A. Yorke, Phys. Rev. E **54**, 71 (1996).
- [8] V. Astakhov, A. Shabunin, W. Uhm, and S. Kim, Phys. Rev. E **63**, 056212 (2001).
- [9] M. Kitano, T. Yabuzaki, and T. Ogawa, Phys. Rev. A **29**, 1288 (1984).
- [10] R. M. Everson, Phys. Lett. A **122**, 471 (1987).
- [11] P. Chossat and M. Golubitsky, Physica D **32**, 423 (1988).
- [12] P. Ashwin, Phys. Lett. A **209**, 338 (1995).
- [13] Y. C. Lai, Phys. Rev. E **53**, R4267 (1996).
- [14] Y. C. Lai, Phys. Rev. E **56**, 1407 (1997).
- [15] T. Kapitaniak, Y. Maistrenko, and S. Popovych, Phys. Rev. E **62**, 1972 (2000).
- [16] S. Kraut and U. Feudel, Phys. Rev. E **66**, 015207(R) (2002).
- [17] J. Foss, A. Longtin, B. Mensour, and J. Milton, Phys. Rev. Lett. **76**, 708 (1996).
- [18] A. N. Pisarchik and B. K. Goswami, Phys. Rev. Lett. **84**, 1423 (2000).
- [19] H. Ishii, H. Fujisaka, and M. Inoue, Phys. Lett. **116A**, 257 (1986).
- [20] C. Grebogi, E. Ott, F. Romeiras, and J. A. Yorke, Phys. Rev. A **36**, 5365 (1987).
- [21] I. Pastor-Díaz and A. López-Fraguas, Phys. Rev. E **52**, 1480 (1995).
- [22] D. M. Vavriv, V. B. Ryabov, S. A. Sharapov, and H. M. Ito, Phys. Rev. E **53**, 103 (1996).
- [23] J. M. González-Miranda, Phys. Rev. E **53**, 5656 (1996).
- [24] S. Yanchuk and T. Kapitaniak, Phys. Rev. E **64**, 056235 (2001).
- [25] C. Sparrow, in *The Lorenz Equations: Bifurcations, Chaos, and Strange Attractors* (Springer-Verlag, New York, 1982).
- [26] For example, $\sigma=10$, $r=203$, and $\beta=8/3$. Please refer to Eqs. (2) for the meaning of these parameters.
- [27] L. M. Pecora and T. L. Carroll, Phys. Rev. Lett. **64**, 821 (1990).
- [28] N. F. Rulkov, M. M. Sushchik, L. S. Tsimring, and H. D. I. Abarbanel, Phys. Rev. E **51**, 980 (1995).
- [29] L. Kocarev and P. Parlitz, Phys. Rev. Lett. **76**, 1816 (1996).
- [30] H. D. I. Abarbanel, N. F. Rulkov, and M. M. Sushchik, Phys. Rev. E **53**, 4528 (1996).
- [31] K. Pyragas, Phys. Rev. E **54**, R4508 (1996).
- [32] N. F. Rulkov, V. S. Afraimovich, C. T. Lewis, J. Chazottes, and A. Cordonet, Phys. Rev. E **64**, 016217 (2001).
- [33] S. C. Venkataramani, B. R. Hunt, E. Ott, D. J. Gauthier, and J. C. Bienfang, Phys. Rev. Lett. **77**, 5361 (1996).
- [34] D. J. Gauthier and J. C. Bienfang, Phys. Rev. Lett. **77**, 1751 (1996).
- [35] C. Grebogi, E. Ott, and J. A. Yorke, Phys. Rev. Lett. **48**, 1507 (1982).
- [36] B. R. Hunt, E. Ott, and J. A. Yorke, Phys. Rev. E **55**, 4029 (1997).
- [37] M. Rosenblum, A. Pikovsky, and J. Kurths, Phys. Rev. Lett. **76**, 1804 (1996).
- [38] S. Boccaletti, J. Kurths, G. Osipov, D. L. Valladares, and C. S. Zhou, Phys. Rep. **366**, 1 (2002).
- [39] Z. Zheng and G. Hu, Phys. Rev. E **62**, 7882 (2000).